NOE-CEST and amine–proton exchange imaging of mouse brain with suppression of MTC effects

Jiadi xu[1,2], Kannie W. Y. Chan[1,2], Xiang Xu[1,2], Nirbhay Yadav[1,2], Guanshu Liu[1,2], Michael T. McMahon[1,2], and Peter C. M. van Zijl[1,2]

[1]*Radiology Department, Johns Hopkins University, Baltimore, MD, United States,* [2]*Kennedy Krieger Institute, Baltimore, MD, United States*

Target audience: Investigators interested in CEST imaging and its application to disease models and endogenous and exogenous CEST agents.

Purpose: Recently, a new CEST scheme, VDMP-CEST [1,2], was developed to perform CEST experiments in a fast approach at single frequency instead of the conventional full Z-spectrum acquisition, i.e. acquiring a series of images as a function of irradiation frequency. The VDMP-CEST scheme is based on a pulsed-RF irradiation scheme with the inter-pulse delay varied between two (or more) separate acquisitions, while the RF pulses and the irradiation frequency are the same. A VDMP-CEST contrast image is generated by subtracting the images acquired at two different inter-pulses delays. Herein, we further improved the applicability of VDMP-CEST. First, we developed a strategy to suppress the MTC inference. Second, we expanded the range of VDMP-CEST detection from the original limit of slowly exchanging protons to also include fast exchanging species, thereby making the VDMP-CEST method suitable for a wide array of applications.

Methods: In the new VDMP-CEST scheme, the images are still generated by subtracting images acquired at two inter-pulse delays, but now so that MTC effects cancel. The first delay is set to zero, and the second delay is chosen so that the MTC signal will be equal to the signal at zero delay, and which is referred as τ_{null} (see Fig. 1).). In contrast, the CEST signal from slowly exchanging protons is positive, while that of the fast exchanging protons is negative, as shown from the Bloch simulations in Fig.1. The current method thus functions as an exchange rate filter, and removes the MTC by its unique exchange rate, which is in the order of 60-100 Hz [1]. Notice that this rate is the one from the semi-solid pool to the large water pool, while the inverse rate from water to the semisolid is usually reported [3]. In the current simulation, the saturation offset was set to 3.6 ppm, which is far from the water resonance and the DS saturation is negligible. When the saturation offset is close to water, the DS saturation will cause CEST signal decay with respect to the mixing time similar to the fast exchanging protons. Therefore, the amine-CEST image is an amine proton weighted image with residual DS contribution.

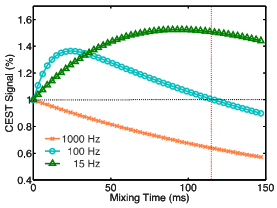

Figure 1. Illustration of the CEST signal as a function of inter-pulse delay for different exchange rates. For clarity, all CEST signal was normalized to the first data point used.

Experiments were performed on a glutamate (Glu) phantom (20 mM) and normal mouse brain. The MRI experiments on mice were conducted on a horizontal 11.7T scanner (Bruker BioSpin). Transmission and detection was achieved using a 23 mm quadrature volume resonator. VDMP-CEST images were acquired using a fast spin echo readout with TR/TE=6 s/5 ms, slice thickness 1 mm, and a 96×96 matrix (FOV 1.6×1.6 cm^2). The τ_{null} depends on the pulse parameters used and was determined by recording the magnetization transfer signal as a function of mixing time at offset 20 ppm. 16 Gaussian shaped RF pulses (270 degree flip angle) with 10 ms pulse width (peak power 4 μT) and τ_{null}=120 ms were used for recording relayed NOE (rNOE-CEST). For recording amine proton exchange images [4], 64 Gaussian shaped RF pulses with 5 ms pulse width (peak power 22 μT, 720 degree flip angle) and τ_{null}=45 ms were applied. The glutamate phantom study was conducted with 128 saturation pulses (Gaussian pulses, pulse width 10 ms, 720 degree flip angle , B1 = 11 μT) at 37°C degree.

Results and Discussion: Typical VDMP-CEST Z-spectra from normal mouse brain acquired at B1 = 11 μT using mixing times zero and τ_{null} = 120 ms are shown in Fig. 2 A (bottom). The difference spectra obtained by subtracting these two Z-spectra are plotted on top. MTC could be well suppressed as evidenced by the difference spectra at offsets >10 ppm and <-10 ppm, which showed intensities close to zero. Fig. 2B shows images obtained at offset -3.5 ppm reflecting relayed NOE signals from the abundant aliphatic groups in mobile proteins and shows weak contrast between white and gray matter. Fig. 2C shows Z-spectra (bottom) and the VDMP difference spectrum (top) at higher power. A large residual intensity is present at -10 ppm, which is due to the broadening of the aliphatic peaks by direct saturation with large bandwidth. The amine proton signal is a mixture of the amine protons of metabolites, such as glutamate (Glu) (see Fig.2E), asparagine (Asn), gamma-aminobutyric acid (GABA), and some residues in mobile proteins such as Lys, Asn and Glu. The contrast of the amine-proton weighted image is similar to the images previously reported in the GluCEST study on mouse brain [5].

Conclusion: The proposed VDMP method can efficiently obtain CEST contrast, both for slow and fast exchange, while significantly suppressing the MTC and direct saturation. Due to the low SAR of the new method, it is also well-suited for implementation on clinical scanners.

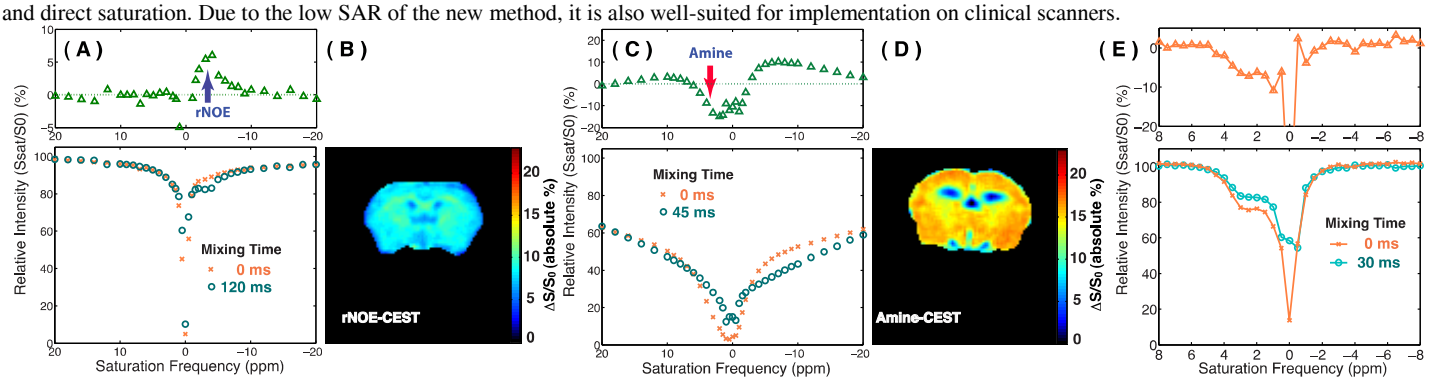

Figure 2. Typical Z-spectra of the VDMP-CEST on a mouse brain with two mixing times using 16 pulse number /360 flip angle (A) and 64 pulse number/720 flip angle (C). Total preparation times are shown at zero delay and τ_{null}. Clean rNOE-CEST image (B) and amine-proton weighted image (D) of the normal mouse brain. (E) Typical VDMP-CEST Z-spectra at two delay times (bottom) and the difference spectrum (top) for a Glu phantom.

References:

1. Xu J et al. MRM DOI: 10.1002/mrm.24850 2. Jones CK et al. Neuroimage 2013;15:114. 3 .Yarnykh, V. L. and C. Yuan NeuroImage 2004, 23: 409. 4. Jin T. NeuroImage 59: 1218. 5. Cai K et al. Nat. Med. 2012;18: 302. **Funding Support:** NIH grants R01EB015031, R01EB015032, P50CA103175, 1S10 RR028955 and P41 EB015909